Scaling of island growth in Pb overlayers on Cu(001)

Wei Li* and Gianfranco Vidali
Department of Physics, Syracuse University, Syracuse, New York 13244-1130

Ofer Biham
Department of Physics, Syracuse University, Syracuse, New York 13244-1130
and Laboratory of Atomic and Solid State Physics, Cornell University, Ithaca, New York 14853
(Received 28 January 1993)

The growth and ordering of a Pb layer deposited on Cu(001) at 150 K has been studied using atom beam scattering. At low coverage, ordered Pb islands with $(\sqrt{61}\times\sqrt{61})R\tan^{-1}\left(\frac{5}{6}\right)$ symmetry are formed. This is a high-order commensurate phase with 30 atoms in the unit cell. From the measurement of the island diffraction peak profiles we find a power law for the mean island size versus coverage with an exponent $n = 0.54 \pm 0.03$. A scaling behavior of growth is confirmed and a simple model describing island growth is presented. Due to the high degeneracy of the monolayer phase, different islands typically diffract incoherently. Therefore, when islands merge they still diffract as separate islands and coalescence effects are thus suppressed. From the result for n we conclude that the island density is approximately a constant in the coverage range $0.1 < \Theta < 0.5$ where the ordered islands are observed [Θ is defined as the ratio between the number of Pb atoms and the number of Cu atoms in the underlying Cu(001) layer]. We thus conclude that most islands nucleate at $\Theta < 0.1$ and then grow in an approximately self-similar fashion as Θ increases.

I. INTRODUCTION

The study of growth and ordering of overlayers deposited on cold single-crystal substrates poses special challenges. Recent experimental[1,2] and computational work[3] on growth of metal overlayers on metal substrates has shown that our understanding of the interplay of kinetic, dynamic, and energetic processes during growth is inadequate. Useful insight may be obtained from studies of the dynamics of nucleation, growth, and coarsening in first-order phase transitions of bulk systems.[4,5] In these studies, a system in thermal equilibrium is quenched into a nonequilibrium state in which two different phases A and B coexist. As a result the system develops spatial inhomogeneities and finally separates into domains of phase A and domains of phase B. The domains of the minority phase typically form isolated droplets inside the majority phase. According to Lifshits and Slyozov,[6] in systems with a constant order parameter the average droplet size $\overline{R}$ increases as a function of time t like

$$\overline{R} \sim t^x, \tag{1}$$

and $x = 1/3$ during the late stages of the growth process. During this process large droplets tend to grow while small droplets evaporate and shrink. The atoms propagate between droplets by diffusion. Similar phenomena on surfaces have recently been studied in the context of adsorbed monolayers.[7,8] In these experiments it was found that $x = 1/3$ in agreement with the theory. In other dynamical phenomena, which occur in systems with a nonconserved order parameter, the growth exponent is $x = 1/2$.[4,5]

Related studies of growth have been done for liquid droplets deposited on a surface at a constant rate.[9–11] It was found that the growth is dominated by two processes. One is the creation of new droplets, while the other is the coalescence of two or more droplets into one larger droplet. The droplets generally extend into the third dimension, and can be approximated as having a spherical shape independent of the size. As a result, when two droplets coalesce into one, the surface area it covers is smaller than the sum of the areas covered by the two droplets. The liquid density on the surface is given by $\rho = rt$, where r is the deposition rate and t is the time. As the deposition proceeds the mean droplet radius increases according to $\overline{R} \sim \rho^n$. However, in the limit of completely flat droplets which do not extend into the third dimension, the power law is modified. This is due to the fact that for flat droplets, the area occupied by a droplet created after coalescence is equal to the sum of the areas of its components, and not smaller. As a result, the mean droplet size increases faster than a power law of ρ. This result also applies to monolayer islands with no internal order. However, as we later show, it does not apply for ordered monolayer phases with high degeneracy (and a large unit cell).

The scaling of island growth in surface adsorption for submonolayer coverage has been studied theoretically and numerically by Bartelt, Evans, and Tringides.[12,13] They used a simple lattice model in which atoms are deposited at a constant rate r and then hop between empty sites as random walkers at a constant rate h. An island is created when an atom reaches a site adjacent to another atom. They then nucleate into a stable island of size two. These islands grow when more atoms reach sites adjacent to them and thus aggregate. Each island in this model, no matter how many atoms it contains, occupies a single site on the lattice. Therefore, this model applies only to the limit of low coverage [up to 0.15 monolayers (ML)], where islands are small and isolated. Using numerical simulations of the model and a rate equation which is

derived from it Bartelt, Evans, and Tringides,[12,13] we find that

$$\overline{S} \sim \Theta^{2/3} D^{1/3}, \tag{2}$$

where $\overline{S}$ is the average number of atoms in an island and $D = h/r$ is the ratio between the hopping rate and deposition rate. If we identify the linear size of an island as $\overline{R} = (\overline{S})^{1/2}$, this result is equivalent to

$$\overline{R} \sim \Theta^{n} D^{\chi}, \tag{3}$$

where $n = 1/3$ and $\chi = 1/6$. The dependence of the average island size on D turns out to be in agreement with the result obtained in Ref. 14 from a completely different approach. Experimental studies in the very low coverage limit are difficult because islands are small and the diffraction signal weak. Thus, evidence of scaling can be found experimentally only over a restricted coverage range.

Quite relevant to our work presented below is the study of growth of ordered Ag islands on Si(111) by Zuo and Wendelken using high-resolution low-energy electron diffraction (HRLEED).[15] They found that the size distribution of islands is self-similar. From an analysis of peak profiles they found that the mean linear size $\overline{R}$ of the islands exhibits a power-law dependence on the coverage Θ of the form

$$\overline{R} \sim \Theta^{n}, \tag{4}$$

where n changes between 0.2 to 0.35 as the substrate temperature is varied from 350 °C to 450 °C. Note that this exponent n is different from the dynamical exponent x of Eq. (1), which is obtained as a function of time for a fixed coverage.

In this paper we present a study of island growth in Pb on Cu(001) at 150 K. We will show that for a slow deposition rate, ordered Pb islands grow according to (4) with $n = 0.54 \pm 0.03$. We will then present a model that interprets our value of the exponent n, indicating that island density is constant during growth within the coverage range explored. The system we study was chosen since it has very intriguing characteristics. First, there is a considerable lattice mismatch (the bulk lattice constant of Cu is 3.6 Å compared to 4.5 Å for Pb). Second, although for deposition at high temperature ($\sim$ 400 K) Pb orders in submonolayer structures, where most of the atoms are in registry with the substrate, at low deposition temperature ($\sim$ 150 K) completely different phases are obtained. At low coverage we observe islands of the $(\sqrt{61}\times\sqrt{61})R\tan^{-1}\left(\frac{5}{6}\right)$ phase. This is a high-order commensurate phase with 30 atoms in the unit cell. The supercell is square, while the proposed internal structure is nearly hexagonal. This phase results from frustration effects, between the adlayer that typically prefers the hexagonal symmetry (which has the largest coordination number) and the underlying square Cu(001) substrate which tends to induce the square symmetry. Near one-layer coverage the $(\sqrt{61}\times\sqrt{61})R\tan^{-1}\left(\frac{5}{6}\right)$ phase disorders and is replaced by a denser monolayer phase with symmetry $(5\times5)R\tan^{-1}\left(\frac{3}{4}\right)$, which is a square phase with 16 atoms in the unit cell.[16]

II. EXPERIMENTAL

The apparatus consists of a helium beam line which is coupled to an ultrahigh vacuum (UHV) chamber.[17] We used a supersonic helium beam of 18.4-meV incident energy, with $\delta v/v \sim 1\%$ velocity resolution with the beam source at 85 K and 1200 psi helium gas pressure. In the UHV chamber there are located a liquid-nitrogen-cooled Knudsen evaporation source, a four-grid low-energy electron diffraction (LEED), Auger optics, and a helium beam detector, which is a differentially pumped quadrupole mass spectrometer with an aperture of 0.5°. This spectrometer can be rotated around the axis of the sample manipulator and can be positioned to measure the reflected helium beam during Pb deposition.[17]

The sample is fixed on a long-travel manipulator with X, Y, and Z translations, and polar and azimuthal rotations. The thoroughly desulfurized copper sample was cleaned prior to each run by Ar-ion sputtering first at room temperature and then at 350 °C. The sample was then annealed at 580 °C and slowly cooled. Helium beam scattering was used to assess the quality of the prepared surface as in previous studies.[2,17]

Pb of 99.999% purity was deposited from a liquid-nitrogen shielded Knudsen evaporation source. The deposition time for one monolayer of Pb was typically about 38 min. The exposure calibration was obtained from Auger Pb and Cu signals and from the analysis of atom beam scattering (ABS) "adsorption curves" (Fig. 1). Somewhat faster deposition rates did not affect the results. Although the layers deposited at 150 K were found to be metastable (see below), there was no indication from ABS, LEED, or Auger of a rearrangement within the layer during measurements.

There is no indication that Pb atoms are incorporated in the Cu crystal. The original Cu(001) surface could be recovered by heating the sample above 580 °C until

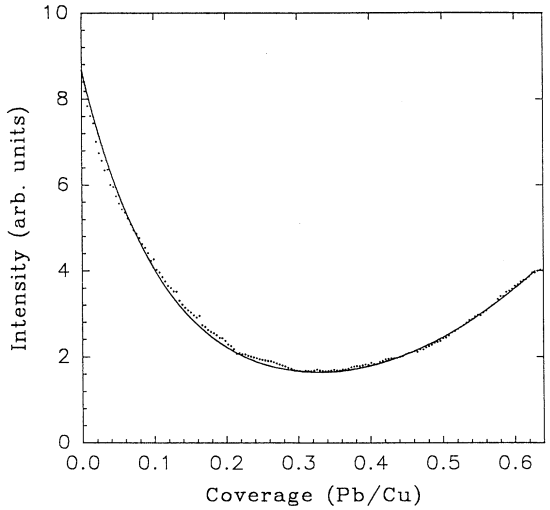

FIG. 1. Pb low-temperature ABS adsorption curve: $I(0,0)$ vs Pb coverage. Surface at 150 K, θ_i=60°. The solid line is a fit to Eq. (5). The coverage is the ratio of the number of Pb atoms to the number of Cu atoms in the Cu(001) layer.

no trace of Pb was left as determined by Auger electron spectroscopy. Furthermore, Pb is virtually immiscible with Cu.[18]

III. RESULTS

A. Characterization of the Pb overlayer

In a previous study,[16] we have used ABS to monitor Pb growth on Cu(001) at low temperature. Here we will describe in more detail how ABS data are used to characterize the growth of a Pb layer. Specifically, we show how the "ABS adsorption curve" (Fig. 1) and the "rocking curve" (Fig. 2) can be used to obtain precise coverage calibration, the average height of Pb adatoms above Cu(001), and the in-phase and/or out-of-phase scattering conditions.

We fit the ABS adsorption curve (Fig. 1) to the equation[19]

$$\frac{I}{I_0} = (1-m\Theta)^{\frac{\Sigma_{\rm Pb} n_s}{m}} + (m\Theta)^{\frac{\Sigma_v n_s}{m}} + 2\left(\frac{A_1}{A_0}\right)\cos\varphi(1-m\Theta)^{\frac{\Sigma_{\rm Pb} n_s}{2m}}(m\Theta)^{\frac{\Sigma_v n_s}{2m}}. \quad (5)$$

The first and the second terms represent scattering from the uncovered parts of the surface and from the adsorbate covered parts, respectively. The last term describes the interference between these contributions. I_0 is the specular peak intensity of the clean surface. The coefficients A_0 and A_1 represent the specular scattering amplitudes: A_0 is from the clean surface while A_1 is the specular peak amplitude at one monolayer completion coverage. The parameter $m = \frac{1}{0.64}$ is the inverse of the ideal coverage for the monolayer completion phase, which is $\Theta = 0.64$ for the $(5\times5)R\tan^{-1}\left(\frac{3}{4}\right)$ phase (see Fig. 3). The coverage Θ is defined as the ratio between the number of Pb adlayer atoms and the number of Cu substrate atoms.

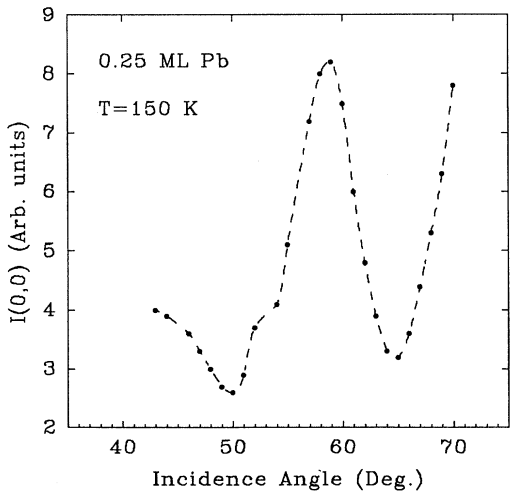

FIG. 2. ABS specular peak intensity vs the incident angle, half-layer Pb deposited. The substrate temperature is T_s = 150 K.

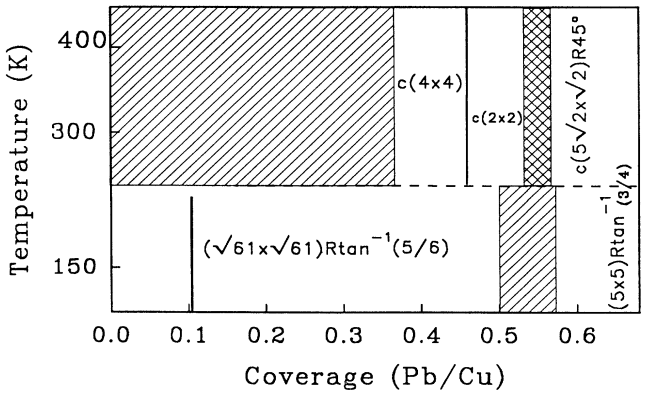

FIG. 3. Sketch of a phase diagram of Pb on Cu(001) obtained by ABS and LEED data. Crossed region: disordered; cross-hatched region: phases coexist.

Thus Fig. 1 can be used to calibrate exposure into coverages. The quantities $\Sigma_{\rm Pb}$ and Σ_v are cross sections of the He-atom scattering from isolated Pb atoms and vacancies in the monolayer, respectively. Figure 1 shows the fitting result (solid line) to the ABS adsorption curve up to one monolayer coverage. From the fitting we have $\Sigma_{\rm Pb}$=58 Å^2 and Σ_v=23 Å^2, respectively. The $\Sigma_{\rm Pb}$ value obtained here is slightly smaller than the 62 Å^2 obtained from fitting to the initial slope of the ABS adsorption curve. The fitted interference factor, $\cos\varphi = 0.99$, gives the phase difference φ between beams reflected from an uncovered surface and the adsorbate overlayer. It is related to the overlayer height by[20]

$$\varphi = 2hk\cos\theta_i + 2n\pi \quad (n, \text{integer}). \quad (6)$$

Here h is the overlayer height, θ_i is the incident beam angle, and k is the beam wave vector which can be obtained by measuring the beam temperature. We obtain that the Pb overlayer height is 2.0±0.1 Å above the Cu plane.

Alternatively, we can obtain the Pb overlayer height by taking a rocking curve, i.e., the ABS specular peak intensity versus the incident angle. Figure 2 shows such a rocking curve taken with a half layer of the $(\sqrt{61}\times\sqrt{61})R\tan^{-1}\left(\frac{5}{6}\right)$ structure (the full layer coverage is 0.49 Pb/Cu atom ratio). The intensity oscillation in Fig. 2 is due to the interference of the scattering from the substrate and Pb layer. Prior to Pb deposition a similar measurement was taken for the clean Cu(001) surface and no oscillations were detected. We have maxima at the in-phase condition and minima at the out-of-phase condition. The following formula:

$$2hk\cos\theta_i = 2n\pi, \quad (7)$$

where n is an integer, gives the in-phase condition. For the half-integer n we have the out-of-phase condition. By analyzing the data in Fig. 2 we obtain that the Pb layer is 2.1 ± 0.1 Å above the Cu(001) surface. This value is in good agreement with the one obtained above by fitting the ABS absorption curve. The above results demonstrate the equivalence of these two methods. Actually,

one can see that they are all based on the interference between specular beams: the reflection from the bare surface and from the deposited overlayer. We have used this information to select the in-phase and out-of-phase conditions for the measurements described in Sec. III C.

B. Low-temperature phases

In Fig. 3 we present a sketch of the phase diagram. The two phases below 0 °C have not been reported by other groups before[21,22] and are obtained after deposition at 150 K. They are likely to be metastable. Upon heating them above about 0 °C they convert into the phases obtained by depositing Pb at 400 K, and they cannot be reached by cooling the overlayer deposited at room temperature. The high-temperature phases are equilibrium phases, since they can be melted and recrystallized.[2,22] We have presented the $(5\times5)R\tan^{-1}\left(\frac{3}{4}\right)$ phase structure elsewhere.[2,16] Here we concentrate on the submonolayer $(\sqrt{61}\times\sqrt{61})R\tan^{-1}\left(\frac{5}{6}\right)$ phase. This phase, as we show in Fig. 3, starts to appear at very low coverage around $\Theta = 0.1$ and continues up to about 0.5 [where Θ is the ratio between the number of adsorbed Pb atoms and the number of Cu atoms in the Cu(001) layer]. The LEED pattern of $(\sqrt{61}\times\sqrt{61})R\tan^{-1}\left(\frac{5}{6}\right)$ turns out to be quite similar to that of $(5\times5)R\tan^{-1}\left(\frac{3}{4}\right)$ (for which $\Theta = 0.64$),[16] and consists of contributions from two types of reciprocal nets. In Fig. 4 the reciprocal lattice nets and proposed structure of $(\sqrt{61}\times\sqrt{61})R\tan^{-1}\left(\frac{5}{6}\right)$ are presented. The two types of reciprocal nets are from two kinds of real space domains as illustrated by two big squares in Fig. 4(b), and are rotated by $\tan^{-1}(5/6)$ and $\tan^{-1}(6/5)$ from the Cu $\langle 1\bar{1}0\rangle$ direction. The LEED spots actually observed are indicated in Fig. 4(a) with dark points, and many of these are from two domains and too close to be resolved. Since the observed LEED pattern is rather faint, the ABS diffraction from this phase (Fig. 5) has played an important role to determine the superstructure. Within the perimeter of the superstructure we propose a compact pseudohexagonal arrangement (30 atoms in the unit cell) with an ideal coverage of 0.49. A similar kind of structure has been proposed before for Bi on Cu(001).[23]

The low-temperature phases are high-order commensurate structures with at most one atom in 16 for the $(5\times5)R\tan^{-1}\left(\frac{3}{4}\right)$ or three atoms in 30 for the $(\sqrt{61}\times\sqrt{61})R\tan^{-1}\left(\frac{5}{6}\right)$ in registry with the substrate. It is unusual to find commensurate structures with so few atoms in registry with the substrate; in fact, in most cases the overlayer structure becomes incommensurate with a hexagonal unit cell. A general procedure for classification

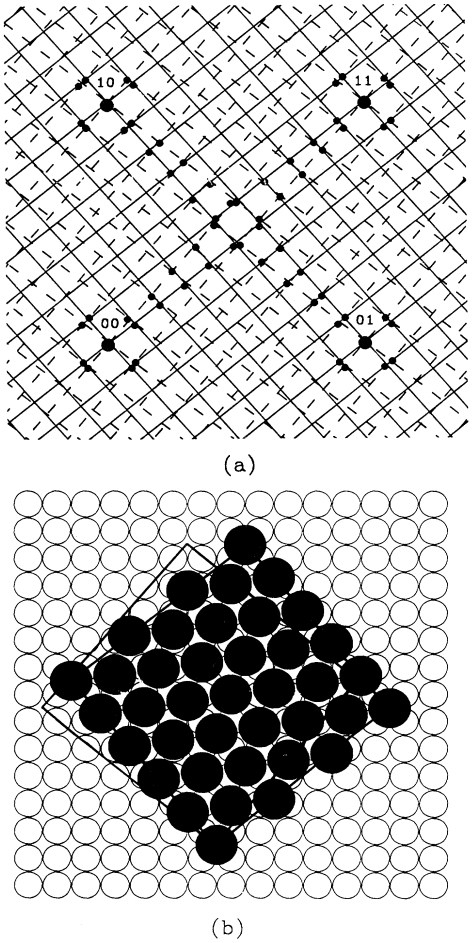

FIG. 4. (a) Reciprocal space: solid and dashed lines are from two domains; (b) proposed real-space structure of $(\sqrt{61}\times\sqrt{61})R\tan^{-1}\left(\frac{5}{6}\right)$. The unit cell which is square contains 30 atoms which are arranged in a pseudohexagonal structure.

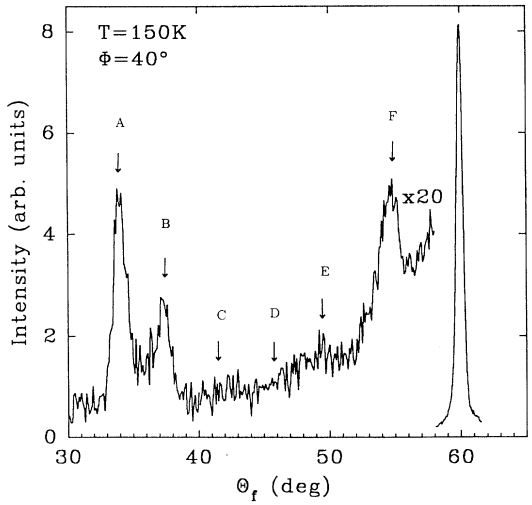

FIG. 5. ABS diffraction scan from $(\sqrt{61}\times\sqrt{61})R\tan^{-1}\left(\frac{5}{6}\right)$, θ_i=60° for full coverage of $\Theta = 0.49$. The substrate temperature is $T_s = 150$ K. We identify the labeling of the peaks as A, (36/61,30/61), (36/61,31/61); B, (30/61,25/61), (31/61,25/61); C, (24/61,20/61); D, (18/61,15/61); E, (12/61,10/61); and F, (6/61,5/61), (5/61,6/61). Note that peaks A, B, and F are double peaks due to overlap between peaks of the two grids. The azimuthal angle Φ is computed from the [110] direction.

of these phases has been proposed,[24] while a calculation of their energetics is in progress.[25]

C. Self-similar growth of Pb islands

As one can see from Fig. 3, the $(\sqrt{61}\times\sqrt{61})R\tan^{-1}\left(\frac{5}{6}\right)$ phase exists at coverages well below its ideal coverage of 0.49, which is an indication of island growth. In Fig. 6 specular peak profiles taken in the nearly in-phase condition are plotted at a few representative Pb coverages. Basically, each peak is composed of two parts: one is the sharp and narrow top peak which is a reflection from an uncovered Cu substrate, and the other is the broadened and shoulderlike tail part which is due to reflection from Pb islands. In the out-of-phase condition, only a broad peak is observed. Although it is possible to extract information on island growth from this measurement, in reality the analysis is complicated by the fact that the ABS specular peak has contributions both from the substrate and islands. In this instance it is far more advantageous to use the ABS diffraction peak due to ordering within Pb islands to investigate how islands grow since there is no interference from the substrate. Figure 7 shows the evolution of the profiles of $(0,-1)$ peak.[26] The decreasing of the peak width with the increasing of the Pb coverage indicates the growth of islands.

The measured peak profiles $I_M(\mathbf{k}_\parallel)$ are actually convolutions of the instrument response function $T(\mathbf{k}_\parallel)$ with the "true" peak shape $I_s(\mathbf{k}_\parallel)$ of the system we are investigating. Two procedures have been applied to extract true peak shapes from

$$I_M(\mathbf{k}_\parallel)=\int T(\mathbf{k}_\parallel-\mathbf{S}_\parallel)I_s(\mathbf{S}_\parallel)d\mathbf{S}_\parallel. \tag{8}$$

First we performed an analysis of the diffraction beam shapes by deconvolving the instrument response function using Fourier analysis. For our ABS system, the instrument response function can be measured by positioning the detector facing the direct incident beam. A small correction, to take into account velocity broadening, has been applied when fitting diffraction peaks. For the best prepared Cu(001) surfaces there is hardly any broadening in the specularly reflected peak. Essentially, what we do is to Fourier transform the measured peaks and the instrument response function (which is a Gaussian). Using the convolution theorem[27] we find that

$$\hat{I}_M(\mathbf{k}_\parallel)=\hat{T}(\mathbf{k}_\parallel)\hat{I}_s(\mathbf{k}_\parallel), \tag{9}$$

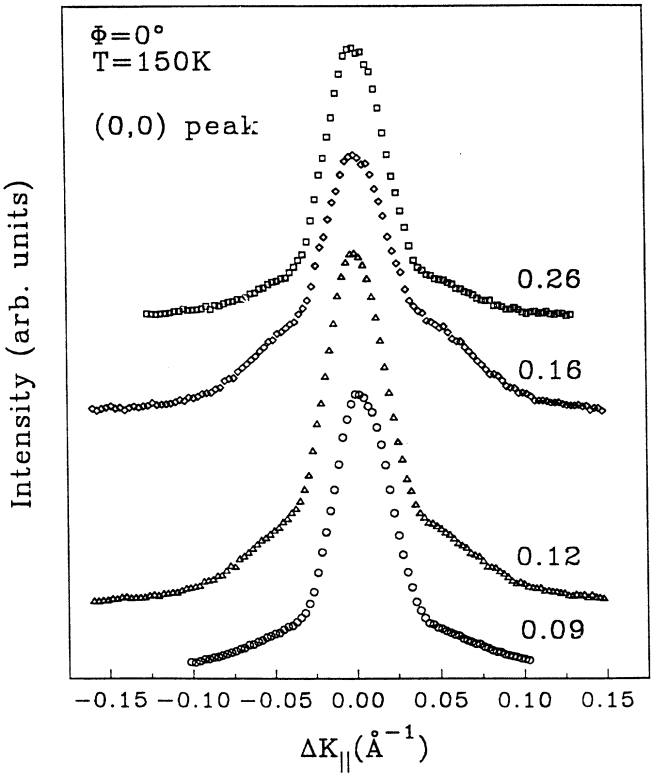

FIG. 6. ABS specular peak profiles at surface temperature of 150 K, θ_i=60° and four values of the coverage Θ. Notice the emergence of wings indicating island growth.

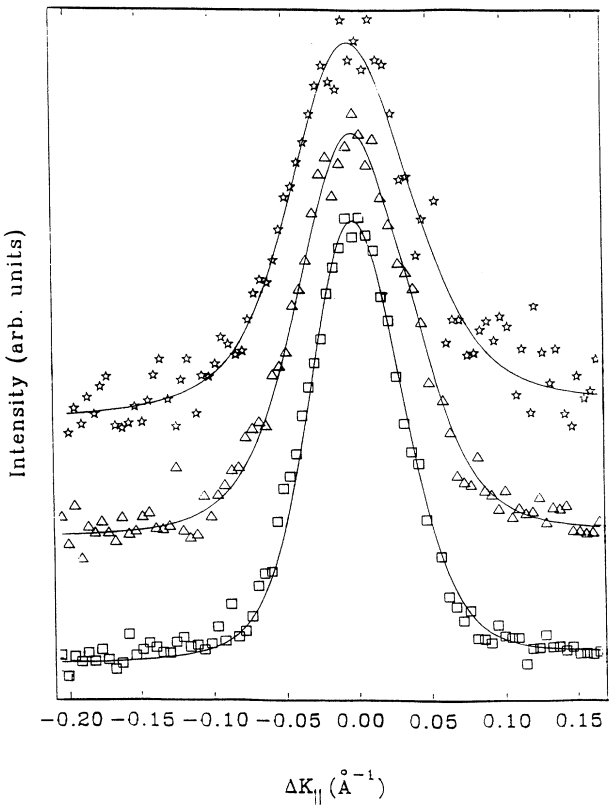

FIG. 7. $(0,-1)$ ABS diffraction peaks from $(\sqrt{61}\times\sqrt{61})R\tan^{-1}\left(\frac{5}{6}\right)$ islands at three representative coverages: Θ = 0.19 (top), 0.29 (middle), and 0.38 (bottom). Solid lines are the fitting results of the convolution of the instrument response function with the function in Eq. (10). The angle θ_i=60°. From the full width at half maximum (FWHM) of such peaks we obtain the scaling of the island size as a function of coverage.

where $\hat{I}_M$, $\hat{T}$, and $\hat{I}_s$ are the Fourier transforms of I_M, T, and I_s, respectively. From this we obtain $\hat{I}_s(\mathbf{k}_\parallel) = \hat{I}_M(\mathbf{k}_\parallel)/\hat{T}(\mathbf{k}_\parallel)$ and then we perform an inverse Fourier transform to get true peak profiles $I_s(k_\parallel)$. The advantage of this process is that these deconvolved data have been obtained without assuming any functional form for the true signal. In Fig. 8 we present deconvolved peak profiles from three representative coverages after normalizing intensities and scaling the horizontal axis. The oscillations in the wings of the peaks are due to the deconvolution procedures; in fact, they are not present in the original data (see Fig. 7). The diffraction profiles represent the structure factor of the physical system. Through our measurement, the different peak profiles coincide with each other after scaling as shown in Fig. 8. In Ref. 28 it is shown that this indicates that the structure factor is a scaling function and is independent of coverage. Thus, we conclude that growth of Pb islands is self-similar in the range of coverage investigated.

To extract quantitative information we proceed as follows. The measured peak profiles are fitted directly by the convolution of the instrument response function (Gaussian) with a chosen function, which is supposed to be the true diffraction peak shape. Following analyses of island growth studied by HRLEED, we tried Gaussian, Lorentzian, and power Lorentzian as fitting functions.[17,29] In Fig. 7, fits using a power Lorentzian

$$I(\Delta K_\parallel) \propto \frac{A}{(\xi^2 + \Delta K_\parallel^2)^m} \tag{10}$$

with $m = 5$ are presented for three different coverages. The same fitting function was used for all coverages, from about $\Theta = 0.1$ to 0.5. The fact that an identical function fits well all the line shapes is again a confirmation of the scaling behavior. However, since there is no theoretical reason to use Eq. (10), it should be considered at this stage only as a convenient fitting function.

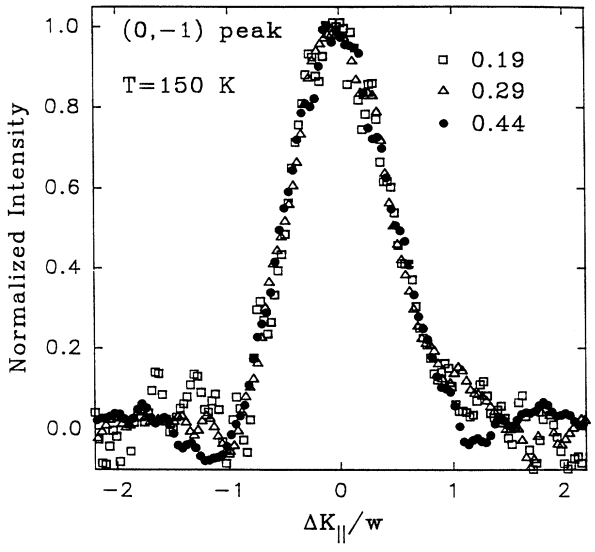

FIG. 8. ABS diffraction data from islands after the deconvolution of the instrument response function. Data from three representative coverages have been rescaled and plot in the same graph. The angle θ_i=60° and w is the full width at half maximum of a peak.

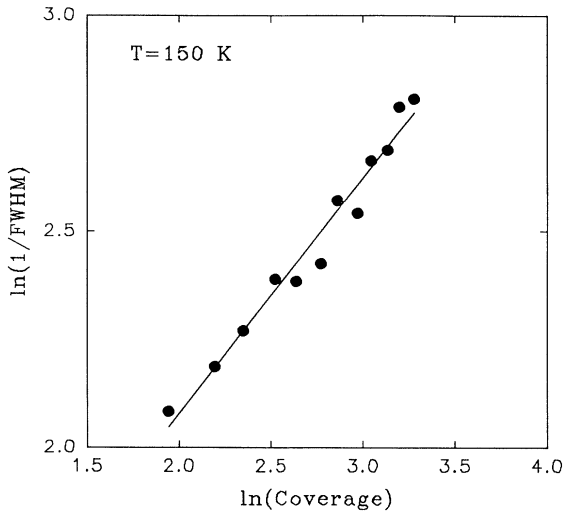

FIG. 9. ln(inverse FWHM) vs ln(coverage) (in arbitrary units) obtained from an analysis of diffraction peaks as in Fig. 7. The line is the best fit through the data, see Eq. (11). The slope is $n = 0.54 \pm 0.03$ for coverage between 0.1 and 0.5.

The inverse width of the deconvolved peak [full width at half maximum (FWHM) of Eq. (10)] is displayed as a function of coverage in Fig. 9. The growth of the mean island size $\overline{R}$ versus coverage can be well described by the equation[15]

$$\overline{R} \sim \frac{1}{\mathrm{FWHM}} \propto \Theta^n. \tag{11}$$

We find that the best fit for the data in Fig. 9 is obtained with $n = 0.54 \pm 0.03$. We estimate that the average

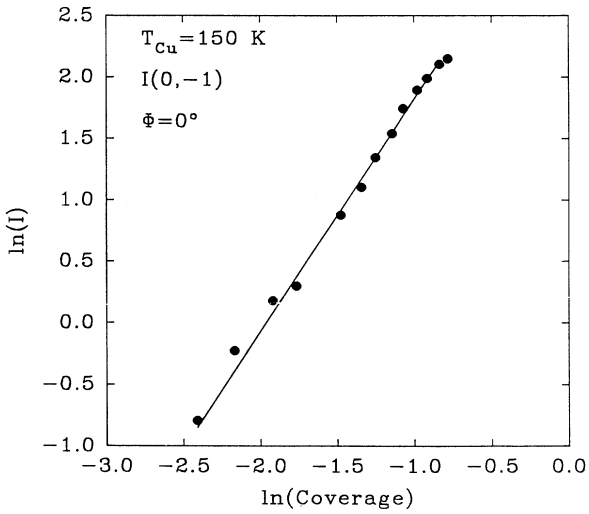

FIG. 10. A ln-ln plot of the $(0, -1)$ peak intensity vs Pb coverage. The solid line is the best-fit to Eq. (12). The slope is $\tilde{p} = 1.89 \pm 0.04$. The units are arbitrary.

size of ordered islands goes from about 50 Å to 120 Å. The value of the exponent we obtain is different from the experiment of Zuo and Wendelken,[15] where n was found to vary between 0.2 at $T = 340\,^{\circ}\mathrm{C}$ and 0.35 at $T = 450\,^{\circ}\mathrm{C}$.

Useful information about island growth and scaling can also be obtained from measurements of diffraction peak intensities. Figure 10 presents our result of the $(0,-1)$ peak intensity as a function of Pb exposure plotted in a ln-ln scale. We can establish a power law by fitting the data in Fig. 10 to

$$I_{01} \sim \Theta^{\tilde{p}}. \tag{12}$$

The solid line in Fig. 10 is the best-fit result, with $\tilde{p} = 1.89 \pm 0.04$.

Note that after a given amount of Pb is deposited we find that the diffraction on specular intensities did not change during data taking (from a few minutes to tens of minutes). This indicates that the layer has stopped evolving before measurements are taken.

IV. DISCUSSION AND INTERPRETATION

To understand the scaling behavior of the islands we first define the island density $N(\Theta)$ which is expected to exhibit a power-law dependence on the coverage

$$N(\Theta) \sim \Theta^{q}. \tag{13}$$

Since the coverage provides the average density of adlayer atoms, which are distributed between islands of various sizes,

$$\Theta \sim N(\Theta)\overline{S}(\Theta), \tag{14}$$

where $S(\Theta) \cong \overline{(R^2)}$ is the average island area. Using the scaling assumption we can write

$$P\big(R(\Theta),\Theta\big) = \frac{1}{\big(\overline{R(\Theta)}\big)^{\lambda}} P'(x), \tag{15}$$

where $P\big(R(\Theta),\Theta\big)$ is the probability, at coverage Θ, of finding an island of size R, $P'(x)$ is a scaling function independent of Θ, and $x = R/\overline{R}$. As a result, we obtain $\overline{(R^2)} \cong (\overline{R})^2$. In this case one can replace Eq. (14) by

$$\Theta \sim N(\Theta)(\overline{R})^2 \sim \Theta^{q+2n}. \tag{16}$$

The scaling assumption thus leads to the relation[15]

$$q + 2n = 1. \tag{17}$$

Submonolayer island growth generally involves two processes in addition to the growth of existing islands: the creation of new islands by nucleation of atoms as the coverage increases and the coalescence of two or more islands into one larger island. The first process tends to increase the island density while the second process decreases it. Typically, in the early stages of growth the islands are very small and isolated, and coalescence is rare. On the other hand, during later growth stages, at relatively high-temperature and low deposition rates, very few new islands form, since mobility is high enough for atoms to aggregate into existing islands. We can thus use Eq. (17) to identify two general regimes of q and n. In systems where islands do not coalesce, their density can only increase, and therefore $q \geq 0$ and $n \leq 1/2$. On the other hand, in cases where islands coalesce but no new islands appear, $q \leq 0$ and $n \geq 1/2$. In systems where both processes occur simultaneously, the values of q and n will be determined by the balance between them.

We will now show that due to the structure of the $(\sqrt{61} \times \sqrt{61})R\tan^{-1}\left(\frac{5}{6}\right)$ phase, coalescence is practically negligible in our system. The phase $(\sqrt{61} \times \sqrt{61})R\tan^{-1}\left(\frac{5}{6}\right)$ has a large unit cell with 30 atoms, only three of them are in perfect registry with the substrate. It thus exhibits a high degeneracy due to both rotations and translations. The supercell can appear with two rotation angles with respect to the substrate: $\theta = \tan^{-1}(5/6)$ or $\theta = \tan^{-1}(6/5)$ (see Fig. 4) and therefore is doubly degenerate. In addition the internal structure of the unit cell can appear in two degenerate states rotated by 90° with respect to each other. The translational degeneracy is due to the large unit cell and the fact that at most three atoms out of 30 can be in perfect registry with the substrate. Careful analysis of the proposed unit-cell structure, which covers 61 lattice sites of the substrate, shows that there are 21 translationally degenerate states. We thus conclude that the total degeneracy in the system is 84-fold. Additional twofold degeneracy appears if these three atoms occupy bridge sites, or fourfold degeneracy appear if none of them occupy a high symmetry site.

The high degeneracy has a substantial effect on the island growth. When two islands start growing into each other and merge it is very unlikely that they will match properly. Since they are degenerate and not in phase they will not diffract coherently. As a result, for our diffraction experiments they behave like separate islands even if physically connected. Therefore, the effects of coalescence are suppressed as far as diffraction measurements are concerned. As a result, the range of values available for q and n is $q \geq 0$ and $n \leq 1/2$. Most of our analysis is based on the $(0,-1)$ diffraction peak, since it is stronger than other peaks and rides over a smooth, constant background. Because this is also a peak reflecting the symmetry of the substrate, according to Henzler[30] the degeneracy is somewhat reduced. However, there is enough degeneracy left to make coalescence effects insignificant almost up to full coverage.

In our experiment $n = 0.54 \pm 0.03$, which is very close to $1/2$. From Eq. (17) we obtain that $q = -0.08 \pm 0.06$, which is close to zero but negative, and may indicate a slight decrease in the island density between $\Theta = 0.1$ and $\Theta = 0.5$. Since we know that there is practically no coalescence in our system we conclude that as the coverage increases between $0.1 < \Theta < 0.5$ no new islands are created and it is thus very close to the marginal case of $q = 0$ and $n = 1/2$. From the relation $\overline{R} \sim \Theta^{n}$ we obtain

$$\frac{d\overline{R}}{d\Theta} \sim \Theta^{n-1} \sim \overline{R}^{(n-1)/n} \tag{18}$$

for the average radius and

$$\frac{d\overline{S}}{d\Theta} \sim \Theta^{2n-1} \sim \overline{S}^{(2n-1)/2n} \tag{19}$$

for the average area. For $n = 1/2$ we find that $d\overline{S}/d\Theta = C$ and C is a constant. This is consistent with a growth model in which the islands are distributed on the surface and each island has an area around it from which it collects the adsorbed atoms.

According to this picture islands are created at low coverage of $\Theta < 0.1$. The dominant mechanism for the creation of new islands seems to occur when two or more atoms meet and nucleate together after deposition.[12,13] Additional islands may appear when atoms nucleate on defects, steps, or impurities on the surface. However, these can account for a small number of islands.

A simple model that may describe the growth process in this system is based on the Voronoi construction.[31] In this construction one first defines a set of points, or centers, on the surface. One then draws the perpendicular bisecting lines to the lines joining any two centers. The smallest convex polygon around each center will contain all the points which are closest to this center. In this model one assumes that an initial distribution of islands is created at very low coverage. As more atoms are deposited, they diffuse and aggregate into existing islands which then grow. Assuming that each atom tends to aggregate into the nearest island, each island attracts the atoms that fall in the Voronoi polygon around it. The size of each island will thus be proportional to the size of the Voronoi polygon around it, at all stages of the growth process. Therefore, within the assumptions of this model, the growth will be self-similar. In reality things are more complicated. Not all deposited atoms aggregate into the nearest island, and most importantly, at larger coverage the important distance is between the deposited atom and the boundary of the island rather than to its initial seed. However, we believe that the island size is proportional to the size of its Voronoi polygon even for high coverage. In numerical simulations for growth of Cu on Cu(001) we find strong evidence in support of this picture.[32] In this system the island density reaches a plateau beyond coverage of a few percent. On this plateau, the islands grow in an approximately self-similar fashion.

Zuo and Wendelken observed that the diffraction peak intensity in their experiment increases like $I \sim \Theta^p$ and also obtained a relation between the exponents n and p with a Γ domain-size distribution. As long as the scaling growth exists, the following relation should be satisfied:[15]

$$p = 1 + 2n. \tag{20}$$

In our experiment we use a linear slit detector which, in fact, integrates over one dimension in k space while the scan is done over the perpendicular direction. Using our power Lorentzian fits we find that the FWHM of our integrated peak scales with Θ exactly like the original peak. However, the integrated peak intensity $I_{01}(k_x)$ scales like the product of the original peak intensity $I_{01}(k_x, k_y)$ and its width (FWHM). Since the width scales like Θ^{-n} we conclude that $\tilde{p} = p - n = 1 + n$. Our result, $\tilde{p} = 1.89 \pm 0.04$, is larger than $1 + n = 1.54 \pm 0.03$. This may be due to the fact that the slit detector is not very sensitive near its ends and thus does not provide a complete integration.

V. SUMMARY

Using ABS, we have studied Pb growth on a Cu(001) substrate at 150 K. Two high-order commensurate phases have been discovered. The $(\sqrt{61} \times \sqrt{61})R\tan^{-1}\left(\frac{5}{6}\right)$ phase has a square unit cell with a proposed quasihexagonal internal structure. This structure seems to be energetically favored since it provides a compromise between the adlayer-adlayer interactions which favor the hexagonal structure and the substrate that tends to induce the square symmetry. We found that the Pb layer grows in $(\sqrt{61} \times \sqrt{61})R\tan^{-1}\left(\frac{5}{6}\right)$ islands before forming the $(5\times5)R\tan^{-1}\left(\frac{3}{4}\right)$ phase which is a square phase. By analyzing line shapes, we are able to show that island growth is self-similar. Power growth laws for mean island size and diffraction peak intensity are established. Due to the high degeneracy of the monolayer phase, when islands merge they form a boundary line. They also do not diffract coherently and therefore coalescence effects are negligible in our diffraction experiments. From the experimental results we conclude that in this particular system, ordered islands tend to form at very low coverage and then grow in an approximately self-similar fashion as the coverage increases. In the future we plan to explore the temperature dependence of the exponents n and $\tilde{p}$, and to examine how the initial island density is determined.

ACKNOWLEDGMENTS

This work was supported by NSF Grants No. DMR-9119735 (G.V.) and No. DMR- 9217284 (O.B.). The work at Cornell (O.B.) was supported by NSF Grants No. DMR-9118065 and No. DMR-9012974. We thank J.-S. Lin and H. Zeng for technical assistance and B. Cooper, T. Curcic, J. Evans, V. Elser, D. Mukamel, J. Sethna, and M. Tringides for helpful discussions.

*Present address: The James Franck Institute, University of Chicago, Chicago, IL 60637.

[1] R. Kunkel, B. Poelsema, L.K. Verheij, and G. Comsa, Phys. Rev. Lett. **65**, 733 (1990); W.F. Egelhoff, Jr. and I. Jacob, *ibid.* **62**, 921 (1989).

[2] Wei Li, J.-S. Lin, M. Karimi, C. Moses, and G. Vidali, J. Vac. Sci. Technol. A **9**, 1707 (1991).

[3] D.E. Sanders and A.E. DePristo, Surf. Sci. **254**, 341 (1991).

[4] J.D. Gunton, M.S. Miguel, and P.S. Sahni, *Phase Transitions and Critical Phenomena*, edited by C. Domb and J.L. Lebowitz (Academic, New York, 1983), Vol. 8, p. 267.

[5] P.C. Hohenberg and B.I. Halperin, Rev. Mod. Phys. **49**, 435 (1977).

[6] I.M. Lifshits and V.V. Slyozov, J. Phys. Chem. Solids **19**, 35 (1961); C. Wagner, Z. Electrochem. **65**, 581 (1961).

[7] M.C. Tringides, Phys. Rev. Lett. **65**, 1372 (1990).

[8]H.-J. Ernst, F. Fabre, and J. Lapujoulade, Phys. Rev. Lett. **69**, 458 (1992).
[9]J.L. Viovy, D. Beysens, and C.M. Knobler, Phys. Rev. A **37**, 4965 (1988).
[10]F. Family and P. Meakin, Phys. Rev. Lett. **61**, 428 (1988).
[11]P. Meakin, Rep. Prog. Phys. **55**, 157 (1992).
[12]M.C. Bartelt and J.W. Evans, Phys. Rev. B **46**, 12 675 (1992).
[13]M.C. Bartelt, M.C. Tringides, and J.W. Evans, Phys. Rev. B **47**, 13 891 (1993).
[14]J. Villain, A. Pimpinelli, and D. Wolf, Comments Cond. Mater. Phys. **16**, 1 (1992).
[15]J.-K. Zuo and J.F. Wendelken, Phys. Rev. Lett. **66**, 2227 (1991).
[16]W. Li, J.-S. Lin, M. Karimi, C. Moses, and G.Vidali, Appl. Surf. Sci. **48/49**, 160 (1991).
[17]G. Vidali, W. Li, J.-S. Lin, and C. Moses, in *Advances in Surface and Thin Film Diffraction*, edited by P. I. Cohen, D. J. Eaglesham, and T. C. Huang, MRS Symposia Proceedings No. 208 (Materials Research Society, Pittsburgh, 1991), p. 99.
[18]M. Hansen and K. Anderko, *Constitutions of Binary Alloys* (McGraw-Hill, New York, 1958).
[19]B. Poelsema and G. Comsa, in *Scattering of Thermal Energy Atoms From Disordered Surfaces*, edited by G. Höhler, Springer Tracts in Modern Physics Vol. 115 (Springer, Berlin, 1989).
[20]W. Li, J.-S. Lin, M. Karimi, P.A. Dowben, and G. Vidali, Phys. Rev. B **45**, 3708 (1992).
[21]A. Sepulveda and G.E. Rhead, Surf. Sci. **66**, 436 (1977).
[22]A. Sánchez and S. Ferrer, Phys. Rev. B **39**, 5778 (1989).
[23]F. Delamare and G.E. Rhead, Surf. Sci. **35**, 172 (1973).
[24]O. Biham, L.-W. Chen, and G. Vidali, Surf. Sci. (to be published).
[25]O. Biham, W. Li, and G. Vidali (unpublished).
[26]Diffraction peaks are labeled according to Fig. 4(a). ABS is sensitive to the top layer only, so there is no contribution from underlying Cu atoms. However, there could be a contribution from clean Cu(001) areas. In reality, recently we observed that, when Pb is adsorbed at 400 K at low coverage ($\Theta \simeq 0.15$), randomly adsorbed Pb atoms produce a change in the composition of the electronic charge-density profile of neighboring Cu atoms yielding a small $(0,-1)$ diffraction peak (Ref 29). Without Pb adsorption the Cu(001) surface is so flat that no diffraction peaks are seen. In the present case this effect is small and confined to the smallest coverages ($\Theta < 0.1$). Thus the $(0,-1)$ diffraction peak is overwhelmingly due to Pb islands. Strong fractional order peaks have been observed, but were not used in the fitting because they were too close to the tails of the dominant $(0,0)$ peak.
[27]I.N. Sneddon, *Fourier Transforms* (McGraw-Hill, New York, 1951).
[28]J.-K. Zuo, Y.-L. He, G.C. Wang, and T.E. Felter, J. Vac. Sci. Technol. A **8**, 2474 (1992).
[29]W. Li and G. Vidali, Phys. Rev. B **46**, 4356 (1992).
[30]M. Henzler, in *Electron Spectroscopy for Surface Analysis*, edited by H. Ibach (Springer-Verlag, Berlin, 1977), p. 117.
[31]See, e.g., D. Weaire and N. Rivier, Contemp. Phys. **25**, 59 (1984).
[32]G. Barkema, O. Biham, M. Breeman, D.O. Boerma, and G. Vidali (unpublished).